# The angle of the near-surface wind-turning in weakly stable boundary layers

Branko Grisogono*
*AMGI, Department of Geophysics, Faculty of Science, University of Zagreb, Croatia*
*Correspondence to: B. Grisogono, University of Zagreb, Geophysics Horvatovac 95, Faculty of Science, Zagreb 10000, Croatia. E-mail: bgrisog@gfz.hr

**The angle between the near-surface and geostrophic wind vector, $\alpha_0$, is discussed in the light of existing and improved Ekman theory and, on the other hand, recently obtained numerical results corroborated by some experimental data, both obtained by other researchers. The latter results for weakly stably stratified boundary layers, also based on large-eddy simulation (LES) data, give an angle that is about $\alpha_0 \approx 35^\circ$. If the Ekman theory is applied slightly above the horizontal surface $z > 0$, for almost any gradually varying eddy diffusivity $K(z)$, which is more realistic than $K = const$ used at $z = 0$ in the classic theory, a closer analytic value to $\alpha_0$ can be provided ($32^\circ$ to $37^\circ$) than that in the classic Ekman theory ($45^\circ$). Alternatively, and without deploying the refined Ekman surface layer theory already suggested here, one may *a priori* use the previously confirmed result, $\alpha_0 \approx 35^\circ$, together with any smooth $K(z)$ in order to find the corresponding surface layer depth. These results, bridging the gap between the existing theory toward fine numerical and limited experimental data, may aid further analyses of weakly stably stratified boundary layers. The information about the angle $\alpha_0$ should be considered in NWP, air-pollution, wind-energy and climate models; otherwise, many important boundary-layer features will remain modelled inadequately.** 

*Key Words:* eddy diffusivity; Ekman layer; meandering; surface layer; WKB theory

*Received 26 March 2010; Revised 13 January 2011; Accepted 13 January 2011; Published online in Wiley Online Library 7 April 2011*

*Citation:* Grisogono B. 2011. The angle of the near-surface wind-turning in weakly stable boundary layers. *Q. J. R. Meteorol. Soc.* **137**: 700–708. DOI:10.1002/qj.789

## 1. Introduction

It has been generally thought and accepted that at least the weakly stably stratified atmospheric boundary layer (SABL) is modelled reasonably well (Nieuwstadt, 1984; Mahrt, 1998; Zilitinkevich *et al.*, 2002; Cuxart *et al.*, 2006; Baklanov and Grisogono, 2007; Mauritsen *et al.*, 2007). However, recent findings show a systematic lack of precision in modelling the angle between the low-level wind and the geostrophic wind, wrong estimates of the SABL depth, being often too high, with a too-weak low-level jet, etc. (e.g. Nielsen and Sass, 2004; Cuxart *et al.*, 2006; Steeneveld *et al.*, 2008; Svensson and Holtslag, 2009), not to mention the understanding and modelling of the SABL itself, and its own details (e.g. Lesieur, 1997; Mahrt, 1998; Mauritsen *et al.*, 2007; Grisogono and Belušić, 2008; Zilitinkevich *et al.*, 2008; Grisogono, 2010). This angle is important for a number of reasons, ranging from detailed weather forecasting and wind energy estimations, to air-pollution modelling and statistics of cyclone lifetimes, etc. For instance, and simplified: too small an angle may yield much too deep a boundary layer, with consequent mixing. Nielsen and Sass (2004) and the websites related to High Resolution Limited Area Model (HIRLAM) reports indicate other effects of the angle on the synoptic surface pressure, etc. At the same time, calculations at the lowest level in our numerical models are often questionable due to simplified lower boundary conditions and the corresponding assumptions considered on the one hand, and often inadequate near-surface vertical resolution on the other (e.g. Mahrt, 1998, 2008a; Beare *et al.*, 2006;

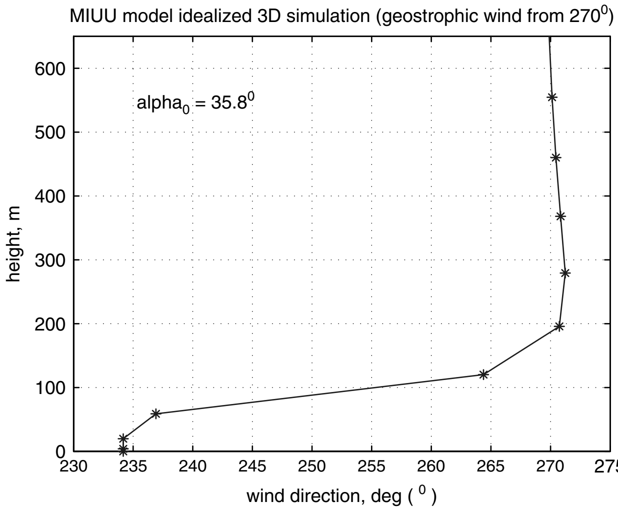


**Figure 1.** Wind direction vs. height from a 3D simulation using the MIUU model by Grisogono and Enger (2004), redone with a finer vertical resolution. The constant input parameters are geostrophic wind (8 m s$^{-1}$, 270°) and stably stratified potential temperature profile, $\Delta\Theta/\Delta z = 5$ K km$^{-1}$. The profile is taken far upstream, in a horizontally stretched grid (vertical grid points marked by stars), several Rossby radii of deformation from an idealized terrain. The corresponding gradient Richardson number increases monotonically upward with its mean for the lowest 100 m equal to 0.22; this corresponds to a weakly stratified SABL. The SABL depth is about 200 m.

van de Wiel *et al.*, 2007; Grisogono and Belušić, 2008). A snapshot of a modelled profile in a weakly stratified SABL is shown in Figure 1 (see later); this is to be distinguished from profiles in strongly stratified SABLs (Mahrt, 1998; Mauritsen *et al.*, 2007; Zilitinkevich *et al.*, 2008; Grisogono, 2010).

The analysis of Svensson and Holtslag (2009; hereafter SH09) shows clearly that an inconsistent or even fully incorrect representation of the near-surface momentum profile in numerical models has a major effect on the angle between the near-surface and geostrophic wind. This has tremendous repercussions on the SABL depth, $H$, and the cross-isobaric mass flux. In their work, SH09 use a multitude of operational and research models vs. LES models, as also explained clearly in e.g. Beare *et al.*(2006) and Cuxart *et al.*(2006). They document that numerical weather prediction (NWP) models usually give: (i) much too deep $H$, (ii) excessive cross-isobaric mass flux, and (iii) too small an angle, $\alpha_0$, between the near-surface and geostrophic wind. The related errors go up to a factor of two or three (SH09). These are serious shortcomings of NWP and models alike, often deliberately made in order to improve the model performances for the sake of large-scale dynamics, such as cyclone filling (e.g. Steeneveld *et al.*, 2008). Since SH09 find that over 40% of the NWP and/or research models fail to reproduce the Ekman spiral ($\alpha_0$ and $H$ in particular), one may only guess which kind of related errors, pertaining to the lack of understanding of the ABL processes and physics of turbulence, appear in climate models functioning at relatively coarser resolutions, or in modelling low-level flows over complex terrain in general. To aid the model analysis mentioned and to corroborate results and discussion of Beare *et al.*(2006), Cuxart *et al.*(2006) and in particular SH09, one of the stated three issues is tackled here, i.e. the angle $\alpha_0$ between the near-surface and geostrophic wind in weakly stratified barotropic horizontal flows. The latter authors show that the typical value of $\alpha_0$ is about 35°. As an illustration of the problem addressed, Figure 1 shows a vertical wind-direction profile from an idealized three-dimensional (3D) simulation using the Meteorologiska Institution, Uppsala Universitet (MIUU) model (Grisogono and Enger, 2004; their section 3e) with a horizontally stretched grid. Based on this Figure, providing the angle between the geostrophic and near-surface wind $\alpha_0 = 35.8°$, this mesoscale model (e.g. Andrén, 1990; Enger, 1990a, 1990b; Tjernström and Grisogono, 2000) may qualify among those research models that followed LES data closely (SH09); in fact, a version of this Swedish model was used in the intercomparison study by Cuxart *et al.*(2006). Since the SABL related to Figure 1 is obtained in a different way, i.e. starting with a stratified environment, than that in Cuxart *et al.*(2006) and SH09, who cooled from below an initially neutral ABL, it appears that the angle $\alpha_0 \sim 35°$ is associated with a larger class of horizontally homogeneous SABL flows.

Curiously enough, van Ulden and Holtslag (1985) obtained similar value for $\alpha_0$ from the experimental data on Cabauw tower in the Netherlands. In general, however, the relevant observations and data analysis pertaining to $\alpha_0$ are very sparse and often inadequate.

Further analysis of the angle of the near-surface wind-turning toward the geostrophic wind, $\alpha_0$, in weakly stratified horizontally homogeneous boundary layers is based on the reasonable assumption that the 'ordinary' SABL can be assessed adequately with the Ekman theory (Pedlosky, 1987; Zilitinkevich *et al.*, 2002; Nielsen and Sass, 2004; SH09). In this approach, seeing a weakly stratified SABL (WSABL) as a generalization of an Ekman layer, a barotropic neutrally stratified layer is gradually cooled from below; this is our WSABL prototype. The well-known 0$^{th}$-order estimation for $\alpha_0$, based on a constant eddy diffusivity value and expansion only up to a first term (in fact, only a limit value for $z \to 0$) gives $\alpha_0$ equal to 45° (e.g. Pedlosky, 1987; Kundu and Cohen, 2002; Nielsen and Sass, 2004; SH09). This value, relying on the classic Ekman-layer theory, is too large compared to the corresponding data, LES and research numerical models (van Ulden and Holtslag, 1985; SH09). A note of caution about Ekman-layer possible instabilities is in order. Although, in principle, the stable Ekman layer may be prone to the inflection point instability (e.g. Brown, 1972), this instability is progressively weaker and eventually disappears at increasing gradient Richardson number, *Ri,* say beyond $Ri > 0.02$ (taken over a small but finite depth) and large Reynolds numbers, *Re*, especially that as in Figure 1 (the simulation goes up to 20 h and there is no sign of any instability). Any plausible growth rates under the corresponding positive *Ri* and very large *Re* considered by van Ulden and Holtslag (1985), Cuxart *et al.*(2006), SH09, and in our Figure 1 would appear vanishingly small or absent. Next, neither of the recent authors reported any sign of the inflection point instability in their WSABL studies; hence, it is believed that this type of instability is largely irrelevant for the range of *Ri* values considered here and very high *Re* (say, $0.1 < Ri < 1$, $Re >> 10^5$). In general, however, this instability cannot be ruled out for all possible WSABL flows.

There are many other important issues and effects related to horizontally homogeneous neutral and WSABL flows. These include, but are not limited to, unsteadiness, baroclinicity, surface conditions, etc. MacKay (1971) studied baroclinic effects in the Ekman-type flows; he speculated that a smaller value than 45° for $\alpha_0$ would be obtained if realistic eddy diffusivity was used. Thompson (1974) dealt with geostrophic shear effects on the near-surface wind, and his range of values for $\alpha_0$ mentions 34°. Mahrt (1974, 1975) assessed time-dependent vertically integrated boundary-layer flows, and advection influence. A recent review and critique of Ekman flows is in Wyngaard (2010).

After the background just presented, the angle $\alpha_0$ will be estimated here based on: (i) the *near*-surface wind with respect to the geostrophic wind, and (ii) the extended theory for almost any gradually varying eddy diffusivity. Within the WKB(J) theory (e.g. Bender and Orszag, 1978; Grisogono, 1995; Grisogono and Oerlemans, 2001a, 2001b; Parmhed *et al.*, 2005), the angle $\alpha_0$ will be shown to largely concur with that from SH09 and van Ulden and Holtslag (1985). To reword, the angle $\alpha_0 \sim 35°$ will be estimated analytically in this study. More importantly, deploying the WKB† theory, additional meaning and use will be given to this angle; this shall be accomplished by smoothly varying eddy diffusivity. If an analytic theory can obtain a result close to that from large-eddy simulation (LES), as will be shown here, the result should be obtainable from our NWP and research models, either by using a finer resolution and/or an improved turbulence parametrization. If they are without this capability of providing a correct $\alpha_0$, many NWP models will not be able to successfully use data assimilation pertaining to the ABL, not to mention the important NWP applications. Overall, all types of near-surface wind simulations and consequent uses require the angle $\alpha_0$ to be modelled as correctly as possible (Nielsen and Sass, 2004; Baklanov and Grisogono, 2007; SH09). To add to the motivation for this study, SH09 show that slightly over 40% of the meteorological models (8 out of 18) used in their study cannot reproduce the Ekman spiral and $\alpha_0$ appropriately (an embarrassing and annoying fact). This paper makes a contribution by tackling the angle $\alpha_0$ in the light of the corresponding and improved Ekman theory for weakly stratified barotropic boundary layers.

## 2. Analytical approach

The 'classical' SABL is almost always stratified weakly (i.e. $Ri << \infty$, typically $0 < Ri < 1$, see e.g. Mauritsen *et al.*, 2007; Zilitinkevich *et al.*, 2008; Grisogono, 2010); hence, its bulk properties have been modelled more or less adequately during the last few decades or so. However, certain assertions about modelling the SABL depth, the low-level jet, the near-surface wind angle with respect to the geostrophic wind, i.e. $\alpha_0$, to mention a few, call for recent and future research (e.g. Cuxart *et al.*, 2006; Grisogono and Belušić, 2008; SH09). Next, we address the angle $\alpha_0$, the surface layer depth and the corresponding eddy diffusivity. Finally, we shall reflect on possible variations of $\alpha_0$ depending on the latter two quantities.

†After the initials of the researchers (Wentzel, Kramers, Brillouin) who popularized this method for solving linear ordinary differential equations, of any order, with variable coefficients.

### 2.1. *Refined estimation of* $\alpha_0$

Here we assess the angle $\alpha_0$ whose tangent is equal to the ratio between the two wind components:

$$\begin{aligned} u(z) &= u_g\{1 - e^{-I(z)}\cos(I(z))\} \\ v(z) &= u_g e^{-I(z)}\sin(I(z)). \end{aligned} \tag{1a}$$

In these textbook expressions, $u_g$ is the geostrophic wind speed, $I(z) = \{f/(2K)\}^{1/2}z$, with $f$ as constant Coriolis parameter and $K$ as eddy diffusivity (e.g. Stull, 1988; Holton, 1992). This $I(z)$ can be interpreted as a dimensionless Ekman layer depth, where the actual depth is normalized by the classical Ekman layer depth (e.g. Pedlosky, 1987; Holton, 1992; Grisogono, 1995). Thus, the angle $\alpha_0$ is:

$$\begin{aligned} \tan(\alpha(z)) &= \frac{v(z)}{u(z)}, \\ \tan(\alpha_0) &= \frac{v_0(z_S)}{u_0(z_S)} \end{aligned} \tag{1b}$$

where all the symbols have their usual meaning (e.g. Pielke, 1984; Stull, 1988); in particular $v(z)$ is the ageostrophic wind component, $u(z)$ is the wind component in the geostrophic wind direction at elevation $z$ above the surface, $\alpha$ is the angle between these components, subscript 's' means a representative near-surface value which we, for convenience, relate to the subscript zero. Within the 0$^{\text{th}}$-order Ekman classic theory (e.g. Pielke, 1984; Kundu and Cohen, 2002; SH09), the tangent of the angle $\alpha_0$ is equal to one, i.e. the idealized value for $\alpha_0$ is, as already mentioned, $\alpha_0 = 45°$. This is quite far away from the observed and recent, best modelled corresponding value in the barotropic WSABL, i.e. $\alpha_0 \approx 35°$ (SH09); therefore, a refined analytic estimate for $\alpha_0$ will be sought. To repeat, within the classic linear theory this angle from (1) becomes:

$$\begin{aligned} \tan(\alpha_0) &= \mathrm{Lim}_{z\to 0}\frac{e^{-I(z)}\sin(I(z))}{1 - e^{-I(z)}\cos(I(z))} \\ &= \mathrm{Lim}_{z\to 0}\left\{1 - I(z) + \frac{2I^2(z)}{3} + \ldots\right\} = 1, \end{aligned} \tag{2a}$$

where $I(z)$ is still simply proportional to $z$ as in and below Eq. (1a), and the functions involved are expanded in their Taylor series. Since we focus on the wind direction in the *near-surface* layer, not through the whole of the boundary layer, this scaling height by $(2K/f)^{1/2}$ seems too large, thus hinting at our approach, i.e. finding a related but refined, smaller vertical scale pertaining to the surface layer only. In this way, one will be able to zoom into the weakly stable surface layer ('stable' always means 'stably stratified'). Note that the straightforward limit in Eq. (2a) leads to the mentioned (too large) classic analytic angle of $\alpha_0 = 45°$. Next, we elaborate on correcting this value.

It is more realistic, and certainly more meaningful for NWP and numerical research models (see SH09 for the models' distinctions), to evaluate Eq. (2a) at a relatively short distance above the surface, say $z_S$, representative for the whole of the surface layer. Such a height should be characterized by blended influences from the flow aloft and the surface immediately below. Because the wind vector at the surface, $\mathbf{v}(z = 0)$, or at the roughness height, does not have a well-defined direction, due to the no-slip lower-boundary condition where the wind speed is zero, it can be imprecise to discuss the angle $\alpha_0$ between the surface wind and geostrophic wind vector. Namely, the angle of zero-vector is undefined by definition; it can be defined only in the limit as $z \to +0$, i.e. from above, but more importantly, we never measure the corresponding surface wind anyway. Hence, we discuss here how to determine the angle $\alpha_0$ between the *near-surface* and geostrophic wind vector. This effectively means expanding Eq. (2a) for a small $z$ bearing in mind the exact $\tan(\alpha_0)$ in Eq. (2a) is a monotonically decreasing function through most of the boundary layer. Since we do not have a general, well-defined way to determine strictly the surface layer depth having two wind components and without involving additional assumptions (by e.g. $z_S \sim 10\%$ of $H$), here we define it as the simplest first minimum of the small-argument polynomial expansion for $v_0(z_S)/u_0(z_S)$ in Eqs (1) and (2). This definition, or better to say, restriction, should also be in accord *a posteriori* with the usual definitions but now involving the ageostrophic wind component as well. Next, we shall elaborate on this surface layer estimate.

Having $f$ fixed, one is left with some relatively small range, pertaining to the surface layer, for the values admitted to the dimensionless depth $I(z) = z\{f/(2K)\}^{1/2}, 0 < I(z) < 1$. For a more mixed, less stratified layer, i.e. the WSABL, having relatively larger representative $K$ values, $z$ may extend to relatively higher corresponding values (always, say, up to about 10% of the WSABL depth, $H$) while keeping the ratio $I(z) = \{f/(2K)\}^{1/2}$ within some acceptable limits to be better defined later. On the contrary, in a progressively more stably stratified, and thus usually less mixed SABL, exhibiting relatively smaller $K$, the corresponding surface layer must inevitably be thinner in order to keep the ratio $z\{f/(2K)\}^{1/2}$ within certain bounds allowed (see below).

For typical values of $K$ and relatively small $z$, e.g. $z_S$, it has been difficult to lower the near-surface angle $\alpha_0$ meaningfully and adequately, so as to correspond to the angles occurring in the observations and state-of-the-art numerical simulations (van Ulden and Holtslag, 1985; SH09). The only assumption here is that the exact ratio $v_0(z_S)/u_0(z_S)$ in Eq. (1b) or (2a), when taken for the small argument $z_S$, can be approximated by a simple polynomial expansion. Next, we focus on the expansion in Eq. (2), beyond its constant term equal to one, for $0 < z_S << H$, i.e.

$$\begin{aligned}\tan(\alpha_0) &= \mathrm{Lim}_{z\to z_S}\frac{\mathrm{e}^{-I(z)}\sin(I(z))}{1-\mathrm{e}^{-I(z)}\cos(I(z))}\\ &= \mathrm{Lim}_{z\to z_S}\frac{\sin(I(z))}{\mathrm{e}^{I(z)}-\cos(I(z))}.\end{aligned} \quad (2b)$$

Now, after sorting out the alike terms, expanding in both the nominator and denominator, and then using the binomial series, one finds in terms of powers of $I(z)$:

$$\begin{aligned}\tan(\alpha_0) &= \mathrm{Lim}_{z\to z_S}\frac{I(z)-\frac{I^3(z)}{3!}+\ldots}{I(z)+I^2(z)+\frac{I^3(z)}{3!}+\ldots}\\ &= \mathrm{Lim}_{z\to z_S}\frac{1-\frac{I^2(z)}{6}+\ldots}{1+I(z)(1+\frac{I(z)}{6})+\ldots}\\ &= \mathrm{Lim}_{z\to z_S}\left\{1-\frac{I^2(z)}{6}+\ldots\right\}\\ &\quad\times\left\{1-I(z)(1+\frac{I(z)}{6})+I^2(z)+\ldots\right\}\\ &= 1-I(z_S)+\frac{2}{3}I^2(z_S)+\ldots\approx P_2(I(z_S)).\end{aligned}$$

Hence,

$$\tan(\alpha_0)\approx P_2(I(z_S)) = 1-I(z_S)+\frac{2}{3}I^2(z_S). \quad (2c)$$

This quadratic expansion $P_2$ in terms of small $I(z_S)$ is sufficient for our purpose, i.e. defining/restricting the surface layer depth in order to eventually refine $\alpha_0$ analytically, from being 45°, lowering $\alpha_0$ closer to 35°. Having involved the ageostrophic wind component, the corresponding simplest polynomial expansion $P_2$, possessing a simple local minimum, for the ratio $v_0(z_S)/u_0(z_S)$ shall be minimized because this $P_2$ is a generally increasing function, while the exact expression for $\tan(\alpha_0)$ in Eq. (2) is a decreasing function. Otherwise, we need to define another measure for how large the argument $I(z)$ should be so that our $P_2$ is a good approximation to the exact ratio. One simple advantage of using $P_2$ is to avoid multiple solutions for its extreme (the minimum). In short, $P_2$ is a good estimate for $\alpha_0$ because $P_2$ follows the actual ratio $\tan(\alpha_0)$ down to its minimum, i.e. the $\min(P_2)$; after this point, $\tan(\alpha_0)$ continues to decrease while $P_2$ begins to grow without a bound. Therefore, we set

$$\begin{aligned}&\tan(\alpha_0)\approx\min\{P_2(I(z_S))\} = \min\left\{1-I(z_S)+\frac{2}{3}I^2(z_S)\right\},\\ &\tan(\alpha_0)\Leftrightarrow\frac{4I(z_S)}{3}-1=0,\Rightarrow\min(I(z_S))=\frac{3}{4},\\ &\tan(\alpha_0)\approx P_2(3/4)=0.625,\Rightarrow\alpha_0=0.5586\Leftrightarrow\alpha_0=32^\circ.\end{aligned} \quad (2d)$$

In this way, a representative dimensionless Ekman surface layer depth, $\min(I(z_S)) = 0.75$, is found in Eq. (2d), which corresponds to $\alpha_{0,\mathrm{ANA}} = 32°$. This refined analytic estimate for $\alpha_0$ is close to that in van Ulden and Holtslag (1985) and SH09, i.e. 35°. A critical view of the value just obtained is in order. The absolute error pertaining to the refined analytic estimation of $\alpha_0$ is more than three times smaller than that using the classic Ekman layer theory (45°). One plots easily the exact ratio $v_0(z_S)/u_0(z_S)$ from Eq. (2) and $P_2$ from Eq. (2c) and sees the curves agree nicely, or adequately, up to the argument about 0.4, or 0.7, corresponding to the angle $\alpha_0 \approx 35°$, or 32°, respectively; this means the only assumption made, $P_2$ being a good approximation here, is acceptable. Since an exact limit up to which a certain series expansion, such as $P_2$, is a valid approximation to an exact function, as in e.g. Eq. (2c), is more or less arbitrary, the simple restriction, based on the simple extreme value of $P_2$, is deployed here.

 

*2.2. Improved surface layer depth*

Because the obtained $\min(I(z_S)) = 0.75$ from Eq. (2d) may seem large, the related $\alpha_{0,ANA} = 32°$ is somewhat smaller than the reference value from van Ulden and Holtslag (1985) and SH09, i.e. 35°. If the Ekman layer depth corresponds to $I(z = H) = 2\pi$, then our newly defined surface layer depth, $\min(I(z_S)) = 0.75$, relates to ∼12% of $H$, which can only be a slight (thus quite acceptable) overestimation. (If a particular calculation would prefer a lower dimensionless Ekman layer depth than $I(z = H) = 2\pi$, then the related value of $I(z_S)$ ought to be reduced accordingly.) Let us compare the new analytic result with the classic Ekman layer and LES results in their dimensionless form. The classic Ekman layer (analytic) result for $\alpha_0 = 45°$, when plugged into Eq. (2), yields the dimensionless Ekman surface layer depth either trivially equal to zero, or $I(z_S) = 1.5$ from $P_2$ in Eq. (2c), clearly a way too high value ($z_{S,CLASSIC} \approx 24\%$ of $H$). When the LES result for $\alpha_0$ (SH09) is plugged in there, two solutions to $P_2$, which is a parabola, appear: $I(z_S) \approx 0.4146$, and $I(z_S) \approx 1.0854$; each of them yields, as expected, $\alpha_0 = 35°$. Moreover, the average value of these two latter solutions to $P_2$ gives our $\min(I(z_S)) = 0.75$. This gives credit to our new independent analytic estimation of the dimensionless Ekman surface layer depth, $I(z_S)$.

Having estimated the surface layer depth $I(z_S)$, a finer analytic revision of the angle $\alpha_0$ may be accomplished. Perhaps an even more realistic value for $\alpha_0$ is reached if the expansion $P_2$ for $\tan(\alpha_0)$ in Eq. (2) is averaged over the dimensionless surface layer depth $0 \leqslant I(z_S) \leqslant 0.75$. The averaging immediately yields $<P_2>= 1/(0.75) \int_0^{0.75} P_2(x)\, dx = x\{1 - x/2 + (2/9)\cdot x^2\}/(0.75)$ evaluated at 0.75 ($x$ is a dummy variable for dimensionless depth) giving $<P_2>= 0.75$; thus, $\alpha_0 = (180^0/\pi)\cdot \mathrm{atan}(0.75) = 36.9°$. Note this value $\alpha_0 = 36.9°$ is even slightly closer to $\alpha_0 = 35°$ obtained in SH09 (than the initial $\alpha_{0,ANA} = 32°$), and that our analytic estimates embrace it now from below and above, i.e. $32° \leqslant \alpha_{0,ANA} \leqslant 36.9°$.

Next, we focus on acceptable values of $z$ and $K$ entering $I(z)$, $0 < z \leqslant z_S$, to see how realistic surface layer estimates are so far. If using only constant $K$ values, $K_C$, then $I_C(z_S) = \{f/(2K_C)\}^{1/2} z_S$ is still inadequate, i.e. unrealistically small in this case. In other words, when using typical constant $K_C$ values in $I_C(z_S)$, reasonable values for $z_S$ cannot be attained. In their Fig. 9, SH09 discuss the WSABL that is usually 180 to 400 m deep (values of $H$, excluding two outliers for simplicity), the optimum depth, corresponding to $\alpha_0 \approx 35°$, being $H \approx 200$ m (also see our Figure 1). Deploying $z_S \sim 10\%$ of $H$ yields $20\ \mathrm{m} \leqslant z_S \leqslant 40$ m. For example, using a typical set of values $(f, K_C, z_S) = (10^{-4}\ \mathrm{s}^{-1}$, $5\ \mathrm{m}^2\mathrm{s}^{-1}$, 30 m), one finds $I_C(z_S) \approx 0.1$, and from Eq. (2c) and $P_2(I(z_S))$ ensues a relatively large angle for this constant $K_C$, i.e. $\alpha_0 \approx 42.2°$.

One may vary this angle somewhat by lowering $K_C$ and increasing $z_S$ values (these should stay within ordinary values for the WSABL), but even the most optimistic estimation can barely reach down to $\alpha_0 \approx 40°$, which is still too high, i.e. close to 45°. Using $\min(I(z_S))$ to adjust $K_C$ and $z_S$ also gives barely realistic values, e.g. $K_C = 1$ or $10\ \mathrm{m}^2\mathrm{s}^{-1}$ gives a surface layer that is 85 or 270 m thick, respectively ($f$ as before). The latter example agrees with the fact that most NWP models exaggerate $H$, and most likely $z_S$ as well (e.g. Cuxart *et al.*, 2006; Steeneveld *et al.*, 2007; SH09). This statement agrees with our earlier suspicion that $(2K_C/f)^{1/2}$ seems too large for the near-surface scaling. Namely, the classical Ekman layer scaling is fine from a large-scale approach, quasi-geostrophic theory in particular (e.g. Pedlosky, 1987; Holton, 1992), yet it is inadequate for scaling near-surface processes (e.g. Berger and Grisogono, 1998). One concludes that the existing theory (Pedlosky, 1987; Zilitinkevich *et al.*, 2002; SH09), executed for $0 < z \leqslant z_S$ and using $K_C$, provides results that are somewhat closer to but still out of reach of the LES and research models' results. In other words, the constant-$K$ approach intrinsically cannot provide acceptable $\alpha_0$ and $z_S$ values.

*2.3. Gradually varying eddy diffusivity K(z)*

Since lowering the angle $\alpha_0$ down from 45° does not allow for realistic pairs of values for $K_C$ and $z_S$ simultaneously in the dimensionless surface layer depth $I(z_S) = \{f/(2K_C)\}^{1/2} z_S$, our next step is a deployment of gradually varying $K(z)$ profiles. A natural generalization of the dimensionless Ekman layer depth, $I(z) = \{f/(2K)\}^{1/2} z$, using a smooth $K(z)$ is the corresponding vertical integration; this relates to a simplified low-order WKB method applied to the Ekman layer. Keeping Eq. (2c) in mind and using almost any form of reasonably smooth $K(z)$, one extends the definition for the dimensionless height:

$$I(z) = \sqrt{\frac{f}{2K}} z \ldots \longrightarrow \ldots \sqrt{\frac{f}{2}} \int_0^z \frac{dz'}{\sqrt{K(z')}} \tag{3}$$

which is the $0^{\text{th}}$-order WKB generalization of the exponent in the Ekman as well as in the Prandtl layer solution (Grisogono, 1995, 2003; Grisogono and Oerlemans, 2001a, 2001b, 2002). Hence, the primary motivation for defining now $I(z)$ as an integral is to obtain the $0^{\text{th}}$-order WKB approximation. An equivalent feature to Eq. (3) is in e.g. linear wave theory, where the dependency on the vertical wave number $m$, that is $\exp(imz)$, is generalized within the WKB theory as $\exp(i \int m(z)\, dz)$, see e.g. Nappo (2002). For simplicity we integrate Eq. (3) from zero elevation, while in a more detailed theory this can be readily done from a given roughness length upwards if necessary (this does not change our main results). To put it in a crude way, Eq. (3) allows for gradual variations of the previously introduced $I(z) = \{f/(2K)\}^{1/2} z$ by simply integrating $K(z)$ vertically (Grisogono, 1995). This is the essence of the WKB method for boundary-layer flows (Bender and Orszag, 1978; Berger and Grisogono, 1998; Parmhed *et al.*, 2005). Now, various reasonably smooth profiles may be deployed in Eq. (3), and one can estimate the corresponding limit Eq. (2c) straightforwardly.

The choice of $K(z)$, i.e. a large class of smooth possible profiles, is addressed here by deploying a simple yet generalized and quite robust form of $K(z)$ which depends on two input parameters only:

$$K(z) = K_0 \frac{z}{h} \exp\left\{-0.5\left(z/h\right)^2\right\}, \tag{4}$$

where $K_0$ relates to the maximum of $K(z)$ as $\max(K(z)) = K_0 e^{-1//2}$ that appears at the elevation $h$, $z_S << h << H$. The latter relative relation among the heights in the WSABL must be fulfilled for the WKB theory to hold; details and applications are in e.g. Parmhed *et al.*(2004, 2005), Grisogono and Belušić (2008), Jeričević and Večenaj

(2009) and Jeričević *et al.*(2010), where Eq. (4) has shown reasonable successes in modelling various types of boundary-layer flows. Briefly, the WKB theory requires that the background, $K(z)$ here, varies on a scale which is (at least somewhat) larger than that for the calculated quantities, i.e. $u(z)$ and $v(z)$; hence $z_S << h$, or at least $z_S < h$. Note that Eq. (4) generalizes the O'Brien third-order polynomial profile (O'Brien, 1970; Grisogono and Oerlemans, 2001a, 2001b; Jeričević *et al.*, 2010); furthermore, it is probably better than any polynomial approximation for $K(z)$ because of its simple analytic properties and its dependence on only two input parameters. Some of the latter authors, as well as Grisogono (2003), checked a couple of polynomial profiles in similar applications, yielding most often qualitatively the same results as with Eq. (4), but demanding more analytical fix-up and/or additional input parameters than with using Eq. (4). For instance, Eq. (4) needs only two input parameters while O'Brien needs four external parameters. Finally, Jeričević *et al.*(2010), using large datasets and numerical modelling, show that Eq. (4) generally performs (at least somewhat) better than the O'Brien profile.

Deploying Eq. (4) as a role model for eddy diffusivity vertical profiles $K(z)$, calculating the dimensionless height $I(z)$ in Eq. (3) one obtains

$$I(z) = \sqrt{\frac{fh}{2K_0}} \int_0^z \frac{\exp\{(z'/2h)^2\}\mathrm{d}z'}{\sqrt{z'}}, \tag{5}$$

which is in fact also a function of $h$ and $K_0$, but for simplicity we assume the latter as external given parameters (see below). Integrating Eq. (5) by parts up to $z_S$, while observing that $z/h \leqslant z_S/h < 1$, one straightforwardly finds the first few, most relevant, terms in Eq. (5). Although an infinite series expansion as the exact solution to Eq. (5) can be written, it suffices here to display only the dominating terms:

$$I(z_S) \approx \sqrt{\frac{2f}{K_0}} \sqrt{h \cdot z_S} \exp\left\{\left(\frac{z_S}{2h}\right)^2\right\} \cdot \left\{1 - \frac{1}{5}\left(\frac{z_S}{h}\right)^2 + \ldots\right\}. \tag{6}$$

The governing effect in Eq. (6) is given by the square-root factors, while the exponential and the rightmost factor together usually amount to up to 1% of typical values of $I(z_S)$; hence we omit these small-correction factors in Eq. (6) and treat it simply as $I(z_S) \approx (2f\ h\ z_S/K_0)^{1/2}$. Note that $I(z_S)$, based on a gradually varying $K(z)$, is different from that for $K_C$.

Next, we estimate typical values of the newly expanded $I(z_S)$ based on Eq. (6), plug it into Eq. (2c) with typical $K$ and $z_S$ values, and compare the angle $\alpha_0$ from this updated theory to the distinct, narrow range of values from the LES data, i.e. $\alpha_{0,\mathrm{LES}}$, presented by SH09 and the observations by van Ulden and Holtslag (1985). For example, starting with a similar typical set of values as before but now adding the height $h$ where $K_0$ is reached, i.e. $(f, K_0, h, z_S) = (10^{-4}\ \mathrm{s}^{-1}$, $5\ \mathrm{m}^2\mathrm{s}^{-1}$, 150 m, 30 m), one now obtains from Eq. (6): $I(z_S) \approx 0.425$ (or 0.424 if simplified as done below Eq. (6)). The latter value when plugged into $P_2$ in Eq. (2d) amounts to $\alpha_{0,\mathrm{APR}} \approx 34.8^\circ$ (or $\alpha_0 = 33.7^\circ$ based on the exact ratio in Eq. (2)). A comment about the choice of $h$, i.e. the level of $\max(K(z))$, follows. The average value of $H$ in SH09 is about $\mathrm{mean}(H) \approx 200$ m, while the median is around 300 m; based on these facts, $z_S$ used in our examples is $z_S \approx 30$ m. Meanwhile, the WKB theory applied to the SABL demands $z_S << h < H$, or at least $z_S < h < H$. Hence, we simply choose here $h \approx 150$ m as a suitable value.

A few tests of robustness for the analytical range of values of $\alpha_0$, i.e. $\alpha_{0,\mathrm{APR}}$, are provided next. Firstly, we should use a somewhat higher value of $K_0$ when comparing our result to the $K_C$ case because the class of profiles chosen in Eq. (4) never reaches the value of $K_0$ but a smaller one, i.e. $K_0 e^{-1//2}$. Hence, let us use a doubled $K_0$, i.e. $10\ \mathrm{m}^2\mathrm{s}^{-1}$, in Eqs (4) and (6), the other values as in the last example; then $I(z_S) \approx 0.30$ and $\alpha_{0,\mathrm{APR}} \approx 37.2^\circ$, based on the polynomial expansion Eq. (2b), or $\alpha_0 \approx 36.8^\circ$, from the corresponding exact ratio. These slightly higher $\alpha_0$ values than those in the previous example appear still quite acceptable for the approximate analytical value of the wind angle $\alpha_{0,\mathrm{APR}}$, and certainly better ones than that obtained by using the $K_C$ approach. Uncertainty estimations of $I(z_S)$ and the angle $\alpha_{0,\mathrm{APR}}$ are aided by realizing and deploying the allowed relative range of values between $z_S$ and $h$, see below Eqs (4) and (5); thus Eq. (6) would be restricted to only two variables, $K_0$ and $z_S$. In particular, parametrizing $h = a\ z_S$ with, say, $4 \leqslant a \leqslant 6$, meaning that $\max(K(z))$ is attained around the middle of the WSABL depth, changes Eq. (6) to:

$$I_a(z_S) \approx \sqrt{\frac{2af}{K_0}} z_S, \tag{6a}$$

where typical acceptable variations of, say, $a \approx 5 \pm 1$ would cause variations in $I_a(z_S)$ within $\sim$10%. Note that the latter parametrization for $h$ also agrees with $z_S \sim H/10$ while roughly $h \sim H/2$. The main result of Eq. (6a), compared to that with $K_C$, is that it provides relatively thinner surface layer depths, $z_S$; these depths are supposed to be more realistic, generally speaking, than those using $K_C$. Hence, Eq. (6a) represents a modified dimensionless Ekman surface layer depth; it is by a factor of $(4a)^{1/2} \sim 4.5$ smaller than that for the classical Ekman layer depth. For example, the ratio between $z_S$ based on the WKB and classic Ekman theory, both for the same $I(z_S)$, amounts to $z_{S,\mathrm{WKB}}/z_{S,C} = (2a^{1/2})^{-1}(K_0/K_C)^{1/2} << 1$ (or at least, $z_{S,\mathrm{WKB}}/z_{S,C} < 1$), for all reasonable choices of $a \geqslant 4$ and yet up to $K_0 \leqslant 15K_C$, depending on the particular values chosen.

To illustrate the advantage of using $K(z)$, as e.g. Eq. (4) or similar, instead of $K_C$, Figure 2 displays two idealized estimations of the weakly stable surface layer depth, $z_S$, based on a chosen $I(z_S) = \{f/(2K_C)\}^{1/2} z_S \approx 0.5$ (constant case, solid) and Eq. (6a), i.e. $I(z_S) \approx I_a(z_S) = \{2af/K_0\}^{1/2} z_S \approx 0.5$ (dashed or dash-dotted). For the latter cases, $a = 5$ and $K_0 = 4K_C$ (dashed) or $K_0 = 2K_C$ (dash-dotted). The main point here is to notice the relation between the surface layer depth $z_S$ for constant and variable eddy diffusivity, respectively (not to dwell on any particular idealized value of $z_S$ even though for, say, $K_C < \sim 5\ \mathrm{m}^2\mathrm{s}^{-1}$, $z_S$ values are very realistic). Note that from Eq. (2c), for this chosen example, $I(z_S) = 0.5$, $P_2(0.5) \approx 0.667$, so that $\alpha_0 \approx 33.7^\circ$ (i.e. close to 35°).

Obviously, even small but still constant eddy diffusivity $K_C$ gives at least doubled surface layer depth compared to that using $K(z)$. Our approach is in agreement with the surface-layer theory where also $K(z) \sim z$ (e.g. Stull, 1988) while minor departures due to, e.g. stability effects (could be included in $K_0$ estimates), do not change our main

 

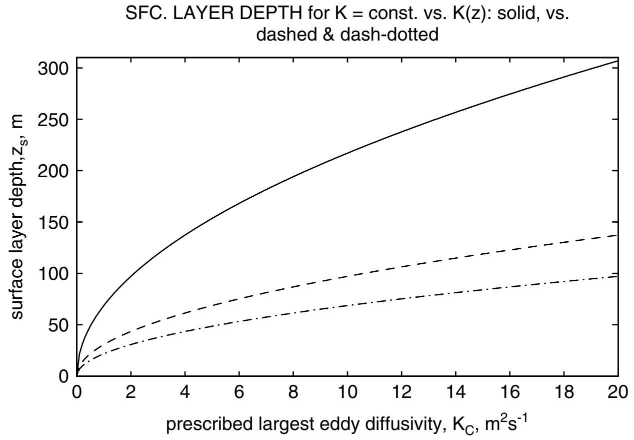


**Figure 2.** Idealized weakly stratified surface layer depth, $z_S$, estimated from eddy diffusivity, based on Eq. (2) and using $I(z_S) = \{f/(2K_C)\}^{1/2} z_S \approx 0.5$ (constant case, solid) and Eq. (6a), i.e. $I_a(z_S) \approx \{2af/K_0\}^{1/2} z_S \approx 0.5$ (gradually varying $K(z)$ using Eq. (4), dashed and dash-dotted). For the latter case, Eq. (4) is used with parametrized $h = a\, z_S$, $a = 5$ and $K_0 = 4K_C$ (dashed) or $K_0 = 2K_C$ (dash-dotted), $f = 10^{-4}\,s^{-1}$. Note realistic $z_S$ values for, say, $K_C < \sim 5\ m^2 s^{-1}$, in this particular example.

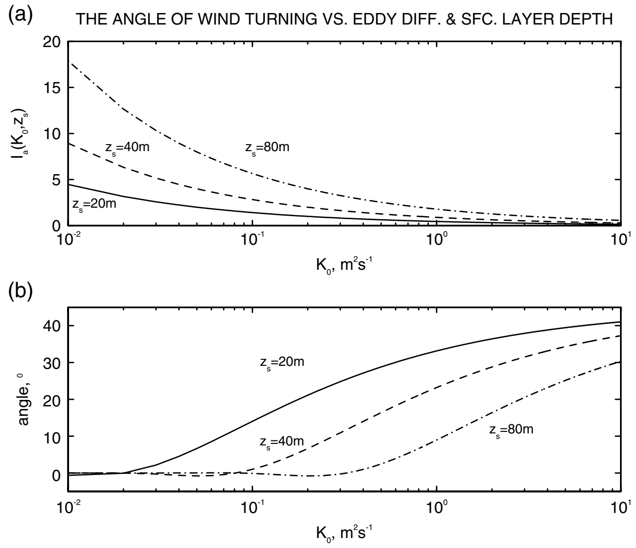


**Figure 3.** Some variations affecting the angle of near-surface wind-turning: (a) the exact argument entering Eq. (2) through Eq. (6) parametrized via Eq. (6a) but now allowing for smooth changes in eddy diffusivity $K_0$; (b) the angle $\alpha_0$ from Eq. (2b), using the exact ratio (not its polynomial expansion $P_2$) as a function of $I_a(K_0, z_S)$. The height of the max($K(z)$) is parametrized as in Eq. (6a) with $h = a\, z_S$, $a = 5$; $I_a(K_0, z_S)$ and $\alpha_0$ are plotted for three different surface layer thicknesses: 20, 40 and 80 m (solid, dashed and dash-dotted, respectively). The latter, deepest, surface layer depth corresponds to a near-neutral surface layer while the former ones relate to weakly stably stratified boundary layers (WSABL).

result. The reader is reminded that many NWP models overpredict the depth of stable surface layers (e.g. Cuxart *et al.*, 2006; Grisogono and Belušić, 2008; SH09; Grisogono, 2010). Finally, we discuss some of the consequences of the analytical approach deployed above, speculate on further applications and summarize the main steps of the paper.

## 3. Discussion and concluding remarks

As an alternative, Eq. (6) can be adopted for estimation of the corresponding attributes ($\alpha_0$ etc.) at the convenient lowest level wind measurement, i.e. at $z_{10m}$ instead of the features at $z_S$. Next, under certain nearly-steady WSABL conditions assumed here, Eq. (6) could be reformulated for estimating $K_0$, or equivalently max($K(z)$), by using Eq. (2) and the requirement that $\alpha_0 \approx 35°$. In other words, by going backward in our analysis, knowing the angle and assuming the overall profile of $K(z)$, some other SABL characteristics can be estimated. Furthermore, using a fine horizontal spacing in a mesoscale network, as in e.g. Belušić and Mahrt (2008), spatial and maybe even temporal variability of the parameters discussed here ($h$, $K_0$, $z_S$, $\alpha_0$) could be assessed.

Before conclusions, a plausible discussion on variations of the angle $\alpha_0$ is tackled. Temporal variations are neglected in section 2; however, these are commonly observed in the SABL and virtually any other ABL (e.g. Mahrt, 1974, 1998, 2008b; Stull, 1988). Forced non-stationarity in a more advanced model than the one used here could yield temporal variations of the angle $\alpha_0$. This may lead toward the unsolved problem of flow meandering and its largely unknown physics (Mahrt, 1998, 2008b; Belušić and Güttler, 2010). In a simplified view, meandering would be given here by temporal variations in $I(z_S)$; as such, qualitatively speaking, temporal variations in Eq. (6) could be foreseen in slowly varying values of $h$, $K_0$ and/or $z_S$. In other words, subtle variations of the surface layer height and eddy diffusivity's maximum value and/or its height, especially those fluctuations in time and perhaps slightly out of phase, will typically cause variations of $I(z)$ in Eqs (5) and (6). According to the polynomial approximation in Eq. (2c), variations of $I(z_S)$, say $\delta I(z_S)$, amounting to e.g. $\pm 30\%$ of $I(z_S)$, will induce variations and some sort of very weak flow meandering at a given location within a few degrees from an average near-surface wind direction. This is too small a directional variation to be considered as meandering because Mahrt (2008b) finds meandering to be directional changes of a few tens of degrees, for wind speeds larger than 1.5 m $s^{-1}$, during typical periods of a few minutes and longer. Nevertheless, we have not yet explored the possibility of qualitatively finding variations of $\alpha_0$ due to larger variations of $I(z_S)$ in the exact form of Eq. (2) without using the polynomial expansion $P_2$ for small argument. These variations may occur even at small elevations $z_S$ if relatively small values are allowed for $K_0$ in Eq. (6) so that the argument entering Eq. (2) may become large.

Possible alterations of the angle $\alpha_0$ caused by variations of the surface layer depth and eddy diffusivity, $z_S$ and $K_0$ respectively, i.e. $\alpha_0(I_a(z_S, K_0))$, are depicted in Figure 3. While Figure 3(a) emphasizes again that small values of $K_0$ may produce large arguments $I_a$, which is basically the same as $I$ entering Eq. (2), even for small near-surface heights $z_S$, Figure 3(b) shows the corresponding variations of the angle $\alpha_0$, thus qualitatively generalizing the approach considered here.

Several conclusions may be drawn from Figure 3. The lower the near-surface elevation (relating to the near-surface wind vector) $z_S$, the lower the corresponding eddy diffusivity yielding the angle $\alpha_0$ that approaches the correct range around $\sim 35°$. Large arguments of $I$ give very small or even slightly negative $\alpha_0$, again in accord with Eq. (2); in the classic Ekman theory, this relates to slightly negative values of the ageostrophic wind component around the top of the (weakly stratified) Ekman layer. If a somewhat larger/lower $a$ value, parametrizing the elevation of max($K(z)$), were used, the same values of $\alpha_0$ would be plotted for slightly smaller/larger heights $z_S$ in Figure 3. For the same value of $z_S$, say 20 m, by gradually changing $0.1\ \mathrm{m^2s^{-1}} \leqslant K_0 \leqslant 0.6\ \mathrm{m^2s^{-1}}$, $\alpha_0$ varies from about 15° to 30°. Moreover, for $z_S = 40$ m and $0.1\ \mathrm{m^2s^{-1}} \leqslant K_0 \leqslant 0.7\ \mathrm{m^2s^{-1}}$, $\alpha_0$ changes between 2° and 20°, or if $0.3\ \mathrm{m^2s^{-1}} \leqslant K_0 \leqslant 5\ \mathrm{m^2s^{-1}}$, then $10^\circ \leqslant \alpha_0 \leqslant 35^\circ$. In a deeper, near-neutral surface layer, Figure 3(b) also suggests the angle $\alpha_0$ may change appreciably as well. For instance, for $z_S = 80$ m, if $0.3\ \mathrm{m^2s^{-1}} \leqslant K_0 \leqslant 3\ \mathrm{m^2s^{-1}}$, then $0^\circ \leqslant \alpha_0 \leqslant 20^\circ$. If a shallower surface-layer were considered, say, $z_S = 10$ m, then minute changes in the range $0.01\ \mathrm{m^2s^{-1}} \leqslant K_0 \leqslant 0.08\ \mathrm{m^2s^{-1}}$, yield $\alpha_0$ variations between 5° and 25° (not shown). The main point of this part of the discussion is to offer a qualitative explanation for one type of simplified meandering, i.e. plausible meandering due to variations in the eddy diffusivity vertical profile (the maximum and its height) and the surface layer depth. Detailed dedicated measurements, similar to those demanded by SH09, are needed in order to further qualify or dispute this hypothesis.

To sum up, while assessing the angle of the near-surface wind-turning in the WSABL, two main things are done here. These are: (i) lifting the height, $z > 0$, where the corresponding angle $\alpha_0$ is evaluated, and (ii) implementing the eddy diffusivity as a gradually varying function of height, $K(z)$. If only the former ingredient is used, based on dimensionless surface layer depth and a quadratic expansion for $\tan(\alpha_0)$, a new analytic estimate is obtained, i.e. $\alpha_0 \sim 35^\circ$, but realistic input values of presumably constant $K$ and stably stratified surface layer depths, $z_S$, are impossible to combine with approximately $32^\circ \leqslant \alpha_0 \leqslant 37^\circ$. When these two ingredients are coupled, i.e. $z = z_S > 0$ and $K(z)$, a reasonable value for $\alpha_0$ ensues (together with realistic $K$ and $z_S$ values) which concurs with that in van Ulden and Holtslag (1985) and SH09, i.e. $\alpha_0 \approx 35^\circ$. In short and to zoom out, the gap between classic Ekman theory, giving too large $\alpha_0 = 45^\circ$ on the one side, and LES and certain observations on the other side, yielding $\alpha_0 \approx 35^\circ$, is bridged by obtaining an asymptotic theoretical value of $\alpha_0 \approx 35^\circ$ as well. Hence, the improved theory (i.e. lifting the height of $\alpha_0$ estimation, and using smooth $K(z)$) adds to the current research by aiming at finding means to reliably lower the SABL depth and its surface layer (e.g. Cuxart *et al.*, 2006; SH09). In this way, a long-standing aspect of the near-surface WSABL behaviour is further elucidated.

## Acknowledgements

Danijel Belušić is thanked for his interest and comments. Larry Mahrt is acknowledged for an extended discussion and broad clarifications. Consequent comments from Sharon Zhong, Leif Enger, Mark Žagar and Robert Banta are appreciated. This study is supported by the Croatian Ministry of Science, Education & Sports, projects BORA No. 119-1193086-1311, and by EMEP4HR project No. 175 183/S30 provided by the Research Council of Norway.

## References

Andrén A. 1990. Evaluation of a turbulence closure scheme suitable for air-pollution applications. *J. Appl. Meteorol.* **29**: 224–239.
Baklanov A, Grisogono B (eds). 2007. Atmospheric boundary layers: Nature, theory and applications to environmental modelling and security. *Boundary-Layer Meteorol.* 125: special issue. Springer: New York.
Beare RJ, MacVean MK, Holtslag AAM, Cuxart J, Esau I, Golaz J-C, Jimenez MA, Khairoutdinov M, Kosovic B, Lewellen D, Lund TS, Lundquist JK, McCabe A, Moene AF, Noh Y, Raasch S, Sullivan PP. 2006. An intercomparison of large-eddy simulations of the stable boundary layer. *Boundary-Layer Meteorol.* **118**: 247–272.
Belušić D, Güttler I. 2010. Can mesoscale models reproduce meandering motions?. *Q. J. R. Meteorol. Soc.* **136**: 553–565.
Belušić D, Mahrt L. 2008. Estimation of length scales from mesoscale networks. *Tellus* **60A**: 706–715.
Bender CM, Orszag SA. 1978. *Advanced Mathematical Methods for Scientists and Engineers*. McGraw-Hill: New York.
Berger BW, Grisogono B. 1998. The baroclinic, variable eddy viscosity Ekman layer: An approximate analytical solution. *Boundary-Layer Meteorol.* **87**: 363–380.
Brown RA. 1972. On the inflection point instability of a stratified Ekman boundary layer. *J. Atmos. Sci.* **29**: 850–859.
Cuxart J, Holtslag AAM, Beare RJ, Bazile E, Beljaars A, Cheng A, Conangla L, Ek M, Freedman F, Hamdi R, Kerstein A, Kitagawa H, Lenderink G, Lewellen D, Mailhot J, Mauritsen T, Perov V, Schayes G, Steeneveld GJ, Svensson G, Taylor P, Weng W, Wunsch S, Xu K-M. 2006. Single-column model intercomparison for a stably stratified atmospheric boundary layer. *Boundary-Layer Meteorol.* **118**: 273–303.
Enger L. 1990a. Simulation of dispersion in moderately complex terrain. Part A: The fluid dynamics model. *Atmos. Environ.* **24A**: 2431–2446.
Enger L. 1990b. Simulation of dispersion in moderately complex terrain. Part C: A dispersion model for operational use. *Atmos. Environ.* **24A**: 2457–2471.
Grisogono B. 1995. A generalized Ekman layer profile with gradually varying eddy diffusivities. *Q. J. R. Meteorol. Soc.* **121**: 445–453.
Grisogono B. 2003. Post-onset behaviour of the pure katabatic flow. *Boundary-Layer Meteorol.* **107**: 157–175.
Grisogono B. 2010. Generalizing '*z*-less' mixing length for stable boundary layers. *Q. J. R. Meteorol. Soc.* **136**: 213–221.
Grisogono B, Belušić D. 2008. Improving mixing length-scale for stable boundary layers. *Q. J. R. Meteorol. Soc.* **134**: 2185–2192.
Grisogono B, Enger L. 2004. Boundary-layer variations due to orographic-wave breaking in the presence of rotation. *Q. J. R. Meteorol. Soc.* **130**: 2991–3014.
Grisogono B, Oerlemans J. 2001a. Katabatic flow: Analytic solution for gradually varying eddy diffusivities. *J. Atmos. Sci.* **58**: 3349–3354.
Grisogono B, Oerlemans J. 2001b. A theory for the estimation of surface fluxes in simple katabatic flows. *Q. J. R. Meteorol. Soc.* **127**: 2725–2739.
Grisogono B, Oerlemans J. 2002. Justifying the WKB approximation in pure katabatic flows. *Tellus* **54A**: 453–462.
Holton JR. 1992. *An Introduction to Dynamic Meteorology*. 3rd edition. *International Geophysics Series*, vol. 48. Academic Press: San Diego.
Jeričević A, Večenaj Ž. 2009. Improvement of vertical diffusion analytic schemes under stable atmospheric conditions. *Boundary-Layer Meteorol.* **131**: 293–307.
Jeričević A, Kraljević L, Grisogono B, Fagerli H, Večenaj Ž. 2010. Parameterization of vertical diffusion and the atmospheric boundary layer height determination in the EMEP model. *Atmos. Chem. Phys.* **10**: 341–364.
Kundu PK, Cohen IM. 2002. *Fluid Mechanics*. 2nd edition. Academic Press: San Diego.
Lesieur M. 1997. *Turbulence in Fluids*. 3rd edition. Kluwer: Dordrecht.
MacKay KP. 1971. Steady state hodographs in a baroclinic boundary layer. *Boundary-Layer Meteorol.* **2**: 161–168.
Mahrt L. 1974. Time-dependent, integrated planetary boundary layer flow. *J. Atmos. Sci.* **31**: 457–464.
Mahrt L. 1975. The influence of momentum advections on a well-mixed layer. *Q. J. R. Meteorol. Soc.* **101**: 1–11.
Mahrt L. 1998. Stratified atmospheric boundary layers and breakdown of models. *Theor. Comput. Fluid Dyn.* **11**: 263–279.
Mahrt L. 2008a. Bulk formulation of the surface fluxes extended to weak-wind stable conditions. *Q. J. R. Meteorol. Soc.* **134**: 1–10.
Mahrt L. 2008b. Mesoscale wind direction shifts in the stable boundary-layer. *Tellus* **60A**: 700–705.
Mauritsen T, Svensson G, Zilitinkevich SS, Esau I, Enger L, Grisogono B. 2007. A total turbulent energy closure model for neutrally and stably stratified atmospheric boundary layers. *J. Atmos. Sci.* **64**: 4113–4126.
Nappo CJ. 2002. *An Introduction to Atmospheric Gravity Waves*. *International Geophysics Series*, vol. 85. Academic Press: San Diego.
Nielsen NW, Sass BH. 2004. '*Rotation of the surface stress as a tool in parameterization of atmospheric turbulence*. Danish Meteorol. Institute, Sci. Rep. 04–07, 25 pp. http://www.dmi.dk/dmi/index/viden/dmi-publikationer/videnskabeligerapporter.htm.
Nieuwstadt FTM. 1984. Some aspects of the turbulent stable boundary layer. *Boundary-Layer Meteorol.* **30**: 31–55.
O'Brien JJ. 1970. A note on the vertical structure of the eddy exchange coefficient in the planetary boundary layer. *J. Atmos. Sci.* **27**: 1213–1215.

 

Parmhed O, Oerlemans J, Grisogono B. 2004. Describing surface fluxes in katabatic flow on Breiðamerkurjökull, Iceland. *Q. J. R. Meteorol. Soc.* **130**: 1137–1151.

Parmhed O, Kos I, Grisogono B. 2005. An improved Ekman layer approximation for smooth eddy diffusivity profiles. *Boundary-Layer Meteorol.* **115**: 399–407.

Pedlosky J. 1987. *Geophysical Fluid Dynamics*. 2$^{nd}$ edition. Springer-Verlag: New York.

Pielke RA. 1984. *Mesoscale Numerical Modeling*. *International Geophysics Series*, vol. 78. Academic Press.

Steeneveld GJ, van de Wiel BJH, Holtslag AAM. 2007. Diagnostic equations for the stable boundary layer height: Evaluation and dimensional analysis. *J. Appl. Meteorol. Clim.* **46**: 212–225.

Steeneveld GJ, Holtslag AAM, Nappo CJ, van de Wiel BJH, Mahrt L. 2008. Exploring the possible role of small-scale terrain drag on stable boundary layers over land. *J. Appl. Meteorol. Clim.* **47**: 2518–2530.

Stull RB. 1988. *An Introduction to Boundary Layer Meteorology*. Kluwer: Dordrecht.

Svensson G, Holtslag AAM. 2009. Analysis of model results for the turning of the wind and related momentum fluxes in the stable boundary layer. *Boundary-Layer Meteorol.* **132**: 261–277.

Thompson RORY. 1974. The influence of geostrophic shear on the cross-isobar angle of the surface wind. *Boundary-Layer Meteorol.* **6**: 515–518.

Tjernström M, Grisogono B. 2000. Simulations of supercritical flow around points and capes in a coastal atmosphere. *J. Atmos. Sci.* **57**: 108–135.

van de Wiel BJH, Moene AF, Steeneveld GJ, Hartogensis OK, Holtslag AAM. 2007. Predicting the collapse of turbulence in stably stratified boundary layers. *Flow Turbul. Combust.* **79**: 251–274.

van Ulden AP, Holtslag AAM. 1985. Estimation of atmospheric boundary layer parameters for diffusion applications. *J. Appl. Meteorol.* **24**: 1196–1207.

Wyngaard JC. 2010. *Turbulence in the Atmosphere*. Cambridge University Press: New York.

Zilitinkevich SS, Baklanov A, Rost J, Smedman A-S, Lykosov V, Calanca P. 2002. Diagnostic and prognostic equations for the depth of the stably stratified Ekman boundary layer. *Q. J. R. Meteorol. Soc.* **128**: 25–46.

Zilitinkevich SS, Elperin T, Kleeorin N, Rogachevskii I, Esau IN, Mauritsen T, Miles MW. 2008. Turbulence energetics in stably stratified geophysical flows: Strong and weak mixing regimes. *Q. J. R. Meteorol. Soc.* **134**: 793–799.

 